# 2016
# ARCCNM / CJK

*July 15, 2016*

*Shenyang, China*

---

**15th Annual General Meeting of the Asian Regional Cooperative Council for Nuclear Medicine**

**7th CJK Conference on Nuclear Medicine**

---

ARCCNM

CSNM

# *Welcome Address*

Dear Colleagues,

On behalf of the Asian Regional Cooperative Council for Nuclear Medicine, welcome to the 15th Annual General Meeting of the ARCCNM held in July 15th, 2016, in Shenyang. I am grateful to Prof. Yaming Li and his team to host this very important Meeting for the Asian nuclear medicine community. I also acknowledge all the participants from all over Asia who sent your scientific and educational abstracts and will present your valuable academic treasures during the Meeting period. Nuclear medicine practice in Asia is now most rapidly growing in the world. We go one more step ahead in Shenyang.

The 3rd Asian Nuclear Medicine Board (ANMB) examination is scheduled on July 14th, 2016, in Shenyang following the first (Osaka) and the second (Jeju) ANMB examination. The 1st Asia Oceania Research Initiative Network (AORIN) Round Table Meeting is initiated on July 16th, 2016, in the same venue. The AORIN project is promoting nuclear practice in your clinic by working together with nuclear medicine–related industries and companies.

Your passion and energy are our fuel. The ARCCNM, the ANMB, the Asian School of Nuclear Medicine, and the AORIN are our engines. I hope you meet old friends and new friends here in Shenyang.

Sincerely yours,

**Jun Hatazawa**

**Chairman**

**Asia Regional Cooperative Council for Nuclear Medicine**

# *Welcome Address*

Dear Colleague:

On behalf of CSNM (Chinese Society of Nuclear Medicine), I am pleased to welcome you to attend the 15th Annual General Meeting of the ARCCNM and the 7th CJK Conference on Nuclear Medicine which will be held from July 14-16, 2016 in Shenyang, China.

The conference is an outstanding Asian forum to present and discuss progress in research, development, standards, and applications of the topics related to nuclear medicine. High quality academic activities will be offered including ARCCNM Symposium, CJK Symposium, Free Paper Session, FANMB Session, Young Investigators Competition and poster session. The Youth Summer Camp of Nuclear Medicine will be held in order to strengthen communication as well as improve the passion and the clinical skills of young nuclear medicine physicians.

I believe you will experience a taste of the Chinese culture in Shenyang which has had the history of over 2300 years. It is an important component of the Chinese culture and education as well as politics and economics. Shenyang is the home of many historic sites including Shenyang Imperial Palace, Zhao Mausoleum (Beiling Park), Fu Mausoleum (Dongling Park), and Zhang's Mansion and places of traditional culture such as Shenyang Zhong Street and Xinbin Manzu Autonomous County.

The 15th Annual General Meeting of the ARCCNM and the 7th CJK Conference on Nuclear Medicine will be a great conference for sharing the latest academic insights as well as experiencing the unique culture of Shenyang, a city that brings the old traditions of China and the new spirit of nuclear medicine.

Thank you for your participation and looking forward to seeing you in Shenyang, China.

Sincerely,

**Yaming Li, MD, PhD, FACNM**
**President of Chinese Society of Nuclear Medicine**
**Professor and Director**
**Department of Nuclear Medicine**
**The First Hospital of China Medical University**

# General Information

## [ Lunch ]

Date & Time: 12:00-13:30, July 15, 2016
Place: Western Dining Room (1F), Sheraton Shenyang South City Hotel

## [ Reception ]

### Welcome Banquet (United Imaging Night)

Date & Time: 18:30-20:30, July 14, 2016
Place: Grand Ballroom (2F), Sheraton Shenyang South City Hotel

### Banquet (Siemens Night)

Date & Time: 19:00-21:00, July 15, 2016
Place: Grand Ballroom (2F), Sheraton Shenyang South City Hotel

## [ Ceremony ]

### Photo Taking of Attendees

Date & Time: 08:30-08:50, July 15, 2016
Place: Backyard, Sheraton Shenyang South City Hotel

### Opening Ceremony

Date & Time: 08:50-09:00, July 15, 2016
Place: Grand Ballroom 1 (2F), Sheraton Shenyang South City Hotel

### Honorary Fellow Award

Date & Time: 13:30-13:35, July 15, 2016
Place: Grand Ballroom 1 (2F), Sheraton Shenyang South City Hotel

### FANMB Certificate Award

Date & Time: 14:00-14:30, July 15, 2016
Place: Room 208/209 (2F), Sheraton Shenyang South City Hotel

## [ Meeting ]

### National Delegate Assembly of ARCCNM

Date & Time: 12:00-13:30, July 15, 2016
Place: Grand Ballroom 1 (2F), Sheraton Shenyang South City Hotel

### CJK Delegate Assembly

Date & Time: 21:00-21:30, July 15, 2016
Place: VIP room of Grand Ballroom (2F)

### Round Table Assembly of AORIN (Asia Oceania Research Initiative Network)

Date & Time: 8:30-12:00, July 16, 2016
Place: Function Room 4 (1F), Sheraton Shenyang South City Hotel

# *Program at a Glance*

| July 14 (Thu) | | | |
|---|---|---|---|
| **Room** | **Lobby** | | |
| 08:00-24:00 | Registration | | |
| 18:00-22:00 | Speakers Ready Table | | |
| 18:30-20:30 | **Welcome Banquet**<br>(United Imaging Night, 2F Grand Ballroom) | | |

| July 15 (Fri) | | | |
|---|---|---|---|
| **Room** | **Grand Ballroom 1 (2F)** | **Room 208/209 (2F)** | **In the back of Grand Ballroom 1** |
| 07:30-08:30 | Breakfast Meeting for ARCCNM Executive Committee<br>(Dining Room, 27F) | | **Poster Exhibition** |
| 08:30-08:50 | **Photo Taking of Attendees** (Backyard) | | |
| 08:50-09:00 | **Opening Ceremony** | | |
| 09:00-10:20 | **ARCCNM Symposium 1. Neurology** | **Free Paper** | |
| 10:20-10:30 | Coffee Break | | |
| 10:30-11:00 | **ARCCNM Symposium 2. Radionuclide Therapy** | | |
| 11:00-12:00 | | **Walking Poster (ANMB)** | |
| 12:00-13:30 | **National Delegate Assembly of ARCCNM**<br>(Lunch) | Lunch<br>(Western Dining Room, 1F) | |
| 13:30-14:00 | **Honorary Fellow Award and Lecture** | | |
| 14:00-15:30 | **CJK Symposium 1. Oncology** | **FANMB Certificate Award and FANMB Session** | |
| 15:30-16:00 | Coffee Break | | |
| 16:00-17:30 | **CJK Symposium 2. General Nuclear Medicine** | **Young Investigators Competition** | |
| 17:30-18:00 | | | |
| 18:00-19:00 | | | |
| 19:00-21:00 | **Banquet**<br>(Siemens Night, 2F Grand Ballroom) | | |
| 21:00-21:30 | CJK Delegate Assembly (VIP Room of Grand Ballroom, 2F) | | |

| July 16 (Sat) | |
|---|---|
| **Room** | **Function Room 4 (1F)** |
| 08:30-12:00 | **Round Table Assembly of AORIN (Asia Oceania Research Initiative Network)** |

# *Scientific Program*

## Grand Ballroom 1 (2F)

08:50 - 09:00 Opening Remark

**09:00 - 10:20 ARCCNM Symposium 1. Neurology**

***Chair:*** *Jun Hatazawa (Japan), Gang Huang (China)*

Clinical Usefulness of Dual Phase F-18 FP-CIT PET Imaging

*Jae Seung Kim (Asan Medical Center, Korea)*

PET Imaging in Parkinson's Disease

*Chuantao Zuo (Huashan Hospital, Fudan University, Shanghai, China)*

New Horizon of Nuclear Medicine in Dementia

*Hiroshi Matsuda (National Center of Neurology and Psychiatry, Tokyo, Japan)*

eZIS Analysis of Brain SPECT in Clinical Routine: A Preliminary Experience of ARCCNM Brain Project in Asia

*Guang-Uei Hung (Chang Bing Show Chwan Memorial Hospital, Changhua County, Taiwan)*

10:20 - 10:30 Coffee Break

**10:30 - 12:00 ARCCNM Symposium 2. Radionuclide Therapy**

***Chair:*** *Henry Bom (Korea), Sijin Li (China)*

Radiobiological Effect and Precision Radiotherapy Monitored Real-time by PET Imaging Products (15O and 11C) of Photomuclear Reactipns in Vivo

*Jun Zeng (Cancer Hospital, Su Zhou University, China)*

PRRT for NET in India

*Partha Choudhury (Rajiv Gandhi Cancer Institute & Research Centre, India)*

Present Status and Strategy to Develop Targeted Radionuclide Therapy (TRT) in Japan

*Seigo Kinuya (Kanazawa University, Japan)*

I-131 Rituximab Radioimmunotherapy

*Ilhan Lim (Korea Cancer Center Hospital, Korea Institute of Radiological and Medical Sciences (KIRAMS), Korea)*

12:00 - 13:30 National Delegate Assembly / Lunch

## *Scientific Program*

**13:30 - 14:00** **Honorary Fellow Award and Lecture**

***Chair:*** *Myung Chul Lee (Korea), Guru Pad Bandopadhyaya (India)*

Award Ceremony

Introduction of Prof. Shizhen Wang

*Yansong Lin (Beijing Xiehe Hospital, CAMS and PUMC, China)*

Nuclear Medicine in China in 2015, A Survey by CSNM

*Yaming Li (The First Hospital of China Medical University, China)*

**14:00 - 15:30** **CJK Symposium 1. Oncology**

***Chair:*** *Yaming Li (China), Byeong-Cheol Ahn (Korea)*

Tyrosine Reporter Gene for Multimodality Imaging

*Xiaoli Lan (Xiehe Hospital, Huazhong Science and Technology University, China)*

Current Updates of PET Oncology

*Keon Wook Kang (Seoul National University, Korea)*

Differential Diagnostic Value of 18F-FDG PET/CT in Patients With Cardiac Tumor

*Ping Gao (Peking University People's Hospital, China)*

Tumor Blood Flow of Lung Cancer Measured By O-15 H2O PET: Pre- and Post-chemotherapy Comparison and Prognosis

*Keiko Matsunaga (Osaka University, Japan)*

15:30 - 16:00 Coffee Break

**16:00 - 17:30** **CJK Symposium 2. General Nuclear Medicine**

***Chair:*** *Hiroshi Toyama (Japan), Hui Wang (China)*

Case-based Discussion: Combination of Functional and Anatomic Imaging for Appropriate Therapy Strategies of Patients With Coronary Artery Diseases

*Jianming Li (TEDA International Cardiovascular Hospital and Tianjin Medical University Cardiovascular Clinical Institute, China)*

Precision Medicine Through Theranostic Nuclear Medicine

*Byeong-Cheol Ahn (Kyungpook National University, Korea)*

Screening, Nuclide Imaging and Targeted Therapy Research of Small Molecular Tumor-inhibitory Peptides Basing on Multiple Targets

*Jie Liu (Southwest Hospital, Third Military Medical University, China)*

Clinical Usefulness of SPECT/CT Scanning- Representative Cases of Daily Clinical Practice

*Hiroshi Toyama (Fujita Health University, Nagoya, Japan)*

## Room 208/209 (2F)

**09:00 - 11:00 Free Paper**

***Chair:*** *Mizanul Hasan (Bangladesh), Lin Li (China)*

A New Method in Production of Macroagreggated Albumin (MAA) Kit

*Farzad Farajbakhsh Mamaghani (PARS ISOTOPE Company, Iran)*

Prediction of Neoadjuvant Radiation Chemotherapy Response and Survival using Pre-treatment [18F] FDG PET/CT Scans in Locally Advanced Rectal Cancer

*Ho-Young Lee (Seoul National University Bundang Hospital, Korea)*

Tumor Response Monitoring using 99mTc-3PRGD2 SPECT-CT in Patients with Her- 2 Positive Breast Cancer

*Bin Ji (China-Japan Union Hospital, China)*

Correlation of 18F-FDG PET/CT Metabolic Parameters with Expressions of ERCC1 and RRM1 in Non-small-cell Lung Cancer

*Na Hu (The Second Xiangya Hospital, Central South University, China)*

99mTc-DPD Scintigraphy and SPECT/CT in Patients with AL and ATTR Type Amyloidosis: Potential Clinical Implications

*Joon Young Choi (Samsung Medical Center, Sungkyunkwan University School of Medicine, Korea)*

Feasibility of Gene-transferred Glucagon-like Peptide 1 Receptor Gene as a Novel Radionuclide Reporter Gene for Molecular Imaging

*Yu Pan (Ruijin Hospital, Shanghai Jiaotong University, China)*

The Study of α4β2 Nicotinic Acetylcholine Receptor Mechanism of Nicotine Administration Attenuates Endothelin-1 Induced Ischemic Cognitive Impairment

*Ruihe Lai (The First Hospital of China Medical University, China)*

11:00 - 12:00 ANMB Walking Poster (In front of the Grand Ballroom)

12:00 - 13:30 Lunch

## *Scientific Program*

**14:00 - 15:30** **FANMB Session**

***Chair:*** *Henry Bom (Korea), Jun Hatazawa (Japan), Durr-e-Sabih (Pakistan)*

FANMB Certificate Award

Development of RAIT Database in Asia Oceania Region

*Zeenat Jabin & Seong Young Kwon (Chonnam National University Hwasun Hospital, Korea)*

Multicenter Clinical Trial of Brain Imaging Using eZIS

*Guang-Uei Hung (Chang Bing Show Chwan Memorial Hospital, Changhua County, Taiwan)*

15:30 - 16:00 Coffee Break

**16:00 - 18:00** **Young Investigators Competition**

***Chair:*** *Raihan Hussain (Bangladesh), Guihua Hou (China)*

The Value of Cingulate Island Sign on Tc-99m ECD Brain SPECT for Discriminating Dementia with Lewy Bodies and Alzheimer's Disease

*Guang-Uei Hung (Chang Bing Show Chwan Memorial Hospital, Changhua County, Taiwan)*

The Selective Internal Radiation Therapy for Liver Cancer with Y-90 Microsphere at Bachmai Hospital

*Pham Cam Phuong (Bach Mai Hospital, Vietnam)*

PET of HER2 Expression with a Novel 18FAl Labeled Affibody

*Yuping Xu (The First School of Clinical Medicine, Nanjing Medical University, China)*

Adenine Nucleotide Translocase2 as a Novel Molecular Determinant of 18F-FDG Accumulation in Various Cancer Cells

*Chul-Hee Lee (Seoul National University, Korea)*

A Novel Peptide Targeting GPC3 for HCC NIR and PET/CT Imaging

*Yushuang Qin (Tongji Hospital, Tongji Medical College, Huazhong University of Science and Technology, China)*

Comparative Study of 99mTc-MDP SPECT/CT Image and Planar Scintigraphy in Assessing Indeterminate Lesion in Diagnosis of Bone Metastasis

*Haoran Hong (The First Hospital of China Medical University, China)*

Asia Oceania Journal of Nuclear Medicine & Biology

# Asia Oceania Journal of Nuclear Medicine & Biology

Volume 4-Supplement 1

# Abstracts

## 15th Annual General Meeting of ARCCNM in conjunction with the 7th CJK Conference on Nuclear Medicine

**July 15th, 2016**

***Shenyang, China***

**Please download the abstract book from**

***http://aojnmb.mums.ac.ir***

**The abstract book is not printed this year and is electronically published (The pdf file is available at: http://aojnmb.mums.ac.ir)**

**AOJNMB is the official publication of Asia Oceania Federation of Nuclear Medicine & Biology and has recently been indexed in Pubmed Central.**

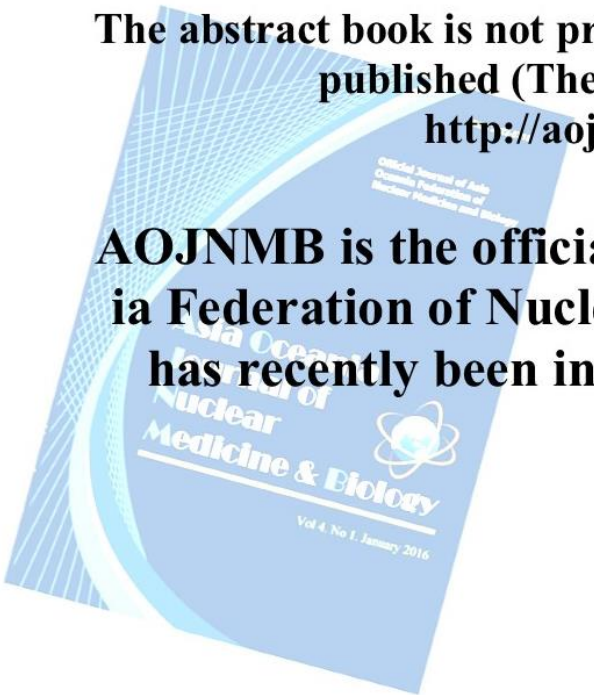


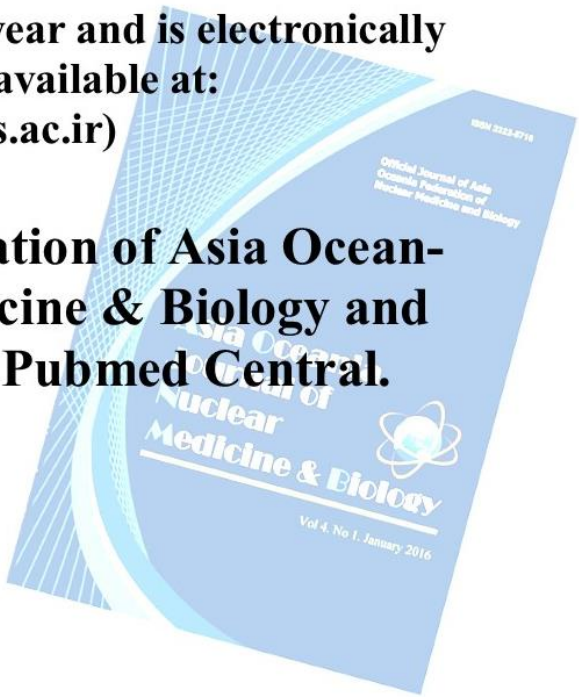

# Additional Abstracts from China

Abstract no. P90 ~ P127

for Poster Presentation

Abstracts which not included in the abstract book

P_90

## Iodine-131 in Helicobacter Pylori Positive Patients: Preliminary Accidental Finding and in Differentiated Thyroid Cancer

Xu Fei, Tang Linglin, Song Shaoli*
*Department of Nuclear Medicine, Renji Hospital Affiliated to Shanghai Jiao Tong University of Medical College, Shanghai 200125, China*

**Objective**: To investigate the eradicate Helicobacter pylori (H. pylori) effect of iodine-131 accidental finding in differentiated thyroid cancer (DTC) patients who underwent 131I therapy.
**Methods**: A total of 130 patients with DTC were underwent iodine-131 treatment. All patients had no stomach-related diseases history. 13C-urea breath test were taken for H. pylori examine before131I treatment. The cutoff value for 13C-UBT was 4‰. For H.P test positive patients, a second 13C-urea test was taken 4 - 6 weeks after 131I treatment. T test were used to compare the difference before and 4 - 6 weeks after iodine-131 treatment.
**Results**: There were a total of 42 of 130(32.31%) subjects were Helicobacter pylori positive. The average value of H. pylori was 28.36‰ before iodine-131, while the value was 18.18‰ after 131I therapy. A significantly decrease in13C-UBT was found after iodine-131 compared with pre-therapy ($p < 0.01$).
**Conclusion**: Our preliminary data demonstrated that iodine-131 has certain eradication effects on Helicobacter pylori, which could provide new approach to multidrug resistance pathogens. In view of the exact molecular mechanism of this phenomenon is still unclear, future clinical applications of this anecdotal finding requires further assessment.

P_91

## A Case of Diffuse B Cell Lymphoma with Bone Metastases and Review of the Literature

Xiaomin Li, Wanchun Zhang*

## Analysis of Clinical Characters in Patients of PCAD with abnormal MPI

Jian Jiao, Mou Tiantian ,Dong Wei, Meng Jingjing, Lu Xia, Wang Qian, Mi hongzhi
*Department of Nuclear Medicine, Beijing Anzhen Hospital, Capital Medical University, Beijing 100029, China*

**Objective**: The aim of this study was to analyze the clinical characters in patients of premature coronary heart disease (PCAD) by myocardial perfusion imaging (The difference results in Laboratory examination, Echocardiography, Clinical symptom, and the character of Coronary artery).
**Methods**: Eighty-three patients of PCAD (determined by coronary angiography in our hospital from January 2015 to January 2016) were included in this study. Fifty-six patients were male and younger than 55 years (y). Twenty-seven patients were female and younger than 65 y. All patients were performed on MPI, and divided into the positive group and the negative group according to the MPI results. The clinical examinations of two groups, such as blood glucose, blood fat, echocardiography, routine blood test, coronary artery and so on were analyzed and compared. Statistical analyses were performed by SPSS 17.0. The measurement data was presented as mean ± standard deviation (SD), and compared using independent sample t-test. The enumeration data was presented as frequency, and compared using chi square test. $P<0.05$ was considered statistically significant.
**Results**: Among those patients (mean age 51.66 ± 6.74), 44 of 83 were positive in MPI, while 39 of 83 were negative. Their average body mass, average body mass index and average uric acid was 75.67 ± 12.52, 26.89 ± 3.47 and 341.16 ± 79.34, respectively. The values of body mass, body mass index and uric acid in the positive group were significant higher than that in the negative group (P=0.008, 0.036 and 0.034, respectively). According to the echocardiography, the patients' average left ventricular ejection fraction (EF), average end-diastolic dimension (EDV) and average end-systolic volume (ESV) was 61.92 ± 7.87, 48.84 ± 5.52 and 32.36 ± 5.92, respectively. The values of EDV and ESV in the positive group were significant higher than that in the negative group (P=0.045, 0.033). The value of left ventricular EF in the positive group was significant lower than that in the negative group (P=0.040). The left anterior descending branch involved most in the vessels of patients of PCAD (68/149=45.9%). Single vessel disease was more often than the other (39/82=47.6%, except one left main disease).
**Conclusions**: The increase of body mass, body mass index and uric acid is related with ischemia in MPI. The EDV, ESV and EF values of echocardiography may offer the information of ischemia. Physicians should pay attention on those clinical characters in patients of PCAD.



## A Case of Relapsing Polychondritis Diagnosis of SPECT-CT

Yuhua Wang, Wanchun Zhang

## Cardiac Function Assement in Patients with Differentiated Thyroid Carcinoma after TSH Suppression Therapy by Gated Myocardial Perfusion Imaging

Ruihua Wang, Shui Jin, xinming Han, Baoping Liu*
*Nuclear Medicine Department, The First Affiliated Hospital of Zhengzhou University, Zhengzhou, Henan province, China*

**Objective(s)**: The aim is to observe cardiovascular dysfunction relation to the duration of therapy and age after TSH suppression treatment in DTC management, including left ventricular diastolic and systolic function, myocardial contractile synchrony, myocardial perfusion, so as to provide theoretical basis for subsequential drug intervention.
**Methods**: The patients were divided into 3 groups by duration of TSH suppression therapy with PTC after thyroid ablation, less than half year, half year to 1 year, more than 1year. The patients were treated as controls who were not received TSH suppression therapy with PTC after thyroid ablation. Gated myocardial perfusion imaging was performed to obtain left ventricular diastolic and systolic function, myocardial contractile synchrony, and myocardial perfusion. The relationship was observed between the duration of therapy and cardiovascular dysfunction after TSH suppression treatment in DTC management.
The patients were divided into 2 groups by 50years old, less than 50years old and more than 50years old. The relationship was observed between the age and cardiovascular dysfunction after TSH suppression treatment in DTC management.
The data was analyzed by SPSS19.0 software. $P < 0.05$ indicates that the difference was statistically significant.
**Results**: 1. Left ventricular diastolic and systolic function EF, PER, PFR, TTPF increased at the half year after TSH suppression treatment, and then decrease by the time. Compared with the control, the p value of EF in the group of more than 1 year was 0.007, the p value of PER in the group of less than half year, more than 1 year was 0.047, 0.010, the p value of PFR in the group of from half to 1 year, more than 1 year was 0.045、0.025. The differences were statistically significant. 2. Myocardial contractile synchrony Phase width, phase standard deviation and entropy had no change in the half year, and increased with the time after half year. Compared with the control, the p value of them was 0.006, 0.007 and 0.001. There was statistically significant. 3. Myocardial perfusion SRS had no change in the first year, and then increased. Compared with the control, the p value of SRS in the group of more than 1 year was 0.000. There was statistically significant. The ratio of perfusion decrease was 50%, 40.91% and 68.75% in the group of less than half year, half to 1year and more than 1year, respectively. 4. There was no statistically significant in every parameters between two group divided by 50years old after more than half year TSH suppression therapy.
**Conclusion**: 1. GMPI can evaluate cardiovascular function in the patients with DTC after TSH suppression therapy from more aspect. 2. TSH suppression therapy induced cardiovascular dysfunction in the patients with DTC. Left ventricular diastolic and systolic function increased at the early time, and then decreased with time. Myocardial contractile synchrony and myocardial perfusion was worsening after 1year of TSH suppression therapy.



## Influence of the First Radioactive Iodine Ablation on Peripheral Complete Blood Count in Patients with Differentiated Thyroid Cancer

Tianpeng Hu MD, Guizhi Zhang MD, Qiang Jia MD, Jian Tan MD, Zhaowei Meng MD PhD*
*Department of Nuclear Medicine, Tianjin Medical University General Hospital, Tianjin, P.R.China*

**Objective**: Radioactive iodine (RAI) is considered to be related with hematologic abnormalities. This study aimed to evaluate influence of the first RAI ablation on peripheral complete blood count (CBC) in patients with differentiated thyroid cancer (DTC).
**Methods**: The data of CBC at baseline and the 6th month were obtained after RAI ablation in 385 DTC patients with approximately 3700 MBq iodine-131. Further comparison was done in 196 patients with available data 1 and 6 months after ablation. The routine blood examination were performed to determine the potential impact of RAI on white blood cell (WBC), red blood cell (RBC), hemoglobin, platelet, neutrophil, lymphocyte and monocyte in both sexes.
**Results**: The first RAI treatment after thyroidectomy was associated with a significant, mild decline in WBC, platelet and lymphocyte that persisted for at least 6 months after ablation. Comparison of the baseline CBC with the follow-up CBC done 6 months later, demonstrated a significant decline in WBC, platelet and lymphocyte without gender differences (all $p<0.05$). Significant rises in RBC and hemoglobin in males and females were found (all $p<0.05$). The decline of platelet in females was more obvious than in males at 100 to 120 mCi of RAI. On the contrary, the rise of RBC and hemoglobin in males was higher than in females. There were no significant clinical complications observed during the follow-up.
**Conclusions**: WBC and platelet decreased continuously from 1 to 6 months after RAI ablation, yet RBC and hemoglobin transiently decreased at 1 month and then increased to levels even higher than baseline.

## Multimodality Imaging in the Mesenteric Castleman's Disease

Shunjun Chen, Bing Cheng, Xingmin Han, Guangjun Niu
*Department of Nuclear Medicine, The First Affiliated Hospital of Zheng Zhou University, China*

**Objective**: To evaluate imaging characteristics of multi-slice·spiral CT(MSCT) and 18F-FDG PET/CT in the patients with the mesenteric Castleman's disease (CD).
**Materials and methods**: A retrospective analysis was made in the MSCT and 18F-FDG PET/CT of 11 patients who were pathologically diagnosed as CD.
**Results**: Imaging findings showed a single mass in 6 patients . The maximum diameter was 6.11±1.45cm. Most were round or oval with equal density, and 3 cases with stippled or branch calcification, and 3 cases were slightly low density, and well defined margins in 10. All patients with the enhancement of the masses had being as strong as the enhancment of aorta at arterial phase and delay scan. Nine patients were seen significantly enhanced tumor blood vessels around the edge or shadow. The degree of 18F-FDG uptake was increasing.11 cases were localized and pathological types were hyaline vascular type.
**Conclusion**: Multimodality imaging performances which had great value for the diagnosis of mesenteric Castleman's disease.



## Experimental Study on the Inhibitory Effect of 131I on Proliferation of Hepatocellular Carcinoma Cells HepG2 saRNA Mediated Regulation of NIS Gene

Juhua Zhuang, Wei XIA*, Jing Ni, Guoyu Wang
*Department of Nuclear Medicine, Shanghai Seventh People's Hospital ,China*

The study was supported by grants from Natural Science Foundation of China (NoNo. 81371597 and No. 81571718)

**Objective**: To explore the feasibility of radionuclide imaging and treatment of Hepatocellular carcinoma induced by transferring small activating RNA (saRNA) mediated sodium iodide symporter ( NIS) gene.
**Methods**: 1.Three saRNA sequences(saRNA-301,saRNA-385 and saRNA-482) for NIS gene were designed and synthesized. 2.The saRNAs were transfected into hepatoma HepG2 cells by using LipofectaminTM2000 as the carrier. 3.The NIS mRNA and protein expression levels were determined by qPCR and Western blotting analysis after 72h. 4.In vitro uptake and efflux of 125I,proliferation inhibition of 131I on HepG2 Cells induced by transferring saRNA-mediated NIS gene were carried out.
**Results**: 1.The saRNA up-regulated the NIS gene expression levels, and the saRNA-482 sequences up-regulated NIS with the highest expression level.. 2.The NIS expression levels reached its peak at 72h after transfection and maintained more than 10 days. 3.There was significantly difference on 125I uptake between transfected cells and non-transfected cells, and the highest uptake of iodine in transfected cells was 64 times higher compared with control cells. 4.Compared with control cells, the growth inhibition rates of 131I on NIS transfected HepG2 cells was 60.7%.
**Conclusion**: The saRNA could upregulate the NIS express levels on hepatocellular carcinoma HepG2 cells and enhance its uptake for radio-iodine. The saRNA-mediated transfer of NIS gene into HepG2 cells might have potential for 131I targeted radiotherapy of hepatocellular carcinoma.

## Risk Factors of Hyperthyroidism with Hepatic Function Injury: A 4-Year Retrospective Study

Chengxia Li, Jian Tan, Guizhi Zhang, Zhaowei Meng, Renfei Wang, Wei Li, Wei Zheng
*Department of Nuclear Medicine, Tianjin Medical University General Hospital, China*

**Objective**: Hepatic function injury is one of the common complications of hyperthyroidism, which affects the choice of treatment and the curative rate. Our goal was to describe clinical and biochemical patterns in patients suffering from Graves' disease (GD) and hepatic function injury and to determine the influential factors.
**Methods**: 1070 patients who received 131I treatment were studied. Many examinations were performed before 131I therapy, such as: the 24-h radioactive iodine uptake of thyroid (RAIU24 h) and serum-free triiodothyronine (FT3), free thyroxine (FT4), sensitive thyroid-stimulating hormone (sTSH), antithyrotrophin receptor antibody (TRAb), thyroglobulin antibody (TgAb), and antithyroid peroxidase antibody (TPOAb), serum hepatic function tests, etc. Data were analyzed by the unpaired t-test, the independent samples t-test, the χ2 test, logistic regression, and Pearson bivariate correlation.
**Results**: Age, course of GD, thyroid's weight, FT4, TPOAb, and TRAb in GD patients with hepatic function injury were higher than those with normal hepatic function patients. The influential factors were age, duration, heart rate, thyroid's weight, FT4, RAIU24 h, TgAb, TPOAb, and TRAb. RAIU24 h was the protecting factor. Age, course of GD, heart rate, thyroid's weight, FT4, TRAb, and TPOAb were the risk factors.
**Conclusion**: Patients whose age was higher than 45yr old, heart rate above 90 bpm, thyroid weight more than 35 g, the duration more than 3 years, FT4 higher than 70.5 pmol/l, the level of TPOAb above 360 IU/ml, and the level of TRAb above 15 IU/l have increased risk of hepatic function injury. As treatment 131I therapy was the best choice.



## Evaluation of the Therapeutic Effectiveness of 131I-EGFR-BSA-PCL in the Colorectal Cancer Mouse Model

Yan-hui Ji , Wei Li , Cheng-xia Li , Zhong-yun Liu, Ning Li, Jian Tan*
*Department of Nuclear Medicine, Tianjin Medical University General Hospital,China*

**Objective**: Colorectal cancer is a highly prevalent and common cancer worldwide. We aimed to investigate the internal irradiation biological effects and therapeutic effectiveness of 131I-labeled anti-EGFR (epidermal growth factor receptor, EGFR) liposomes, derived from cetuximab, were used as a tumor-targeting carrier in colorectal cancer mice models.
**Methods**: We described the liposome, which was characterized for EGFR-targeted binding, and cellular uptake in EGFR-overexpressing LS180 colorectal cancer cells. After intra-tumor injections of 74 MBq (740 MBq/ml) 131I--EGFR-BSA-PCL, we investigated the internal irradiation biological effects and therapeutic efficacy of 131I--EGFR-BSA-PCL in colorectal cancer in a male BALB/c mice model. Tumor size, body weight, histopathology, and SPECT imaging were monitored for 33 d post-therapy.
**Results**: The rapid radioiodine uptake of 131I-EGFR-BSA-PCL and 131I--BSA-PCL reached maximum levels at 4 h after incubation, and the 131I- uptake of 131I-EGFR-BSA-PCL was higher than that of 131I-BSA-PCL in vitro. The 131I tissue distribution assay revealed that 131I-EGFR-BSA-PCL was markedly taken up by the tumor. Furthermore, the tissue distribution assay revealed that 131I-EGFR-BSA-PCLwas markedly taken up by the tumor and reached its maximal uptake value of 21.0±1.01%ID/g-1 (%ID/g is percentage injected dose per gram of tissue) at 72h after of the therapy, the drug concentration in tumor was obviously higher than that in liver, heart, colon, and spleen, respectively. Tumor size measurements showed that tumor development was significantly inhibited by treatments with 131I-EGFR-BSA-PCL and 131I-BSA-PCL. The volume of tumor increased; and treatment rates with 131I-EGFR-BSA-PCL were 124%±7%, lower than with 131I-BSA-PCL (127%±9%), 131I (143%±7%), and normal saline (146%±10%). The percentage losses in original body weights were 39%±3%, 41%±4%, 49%±5%, and 55%±13%, respectively. The best survival and cure rates were obtained in the group treated with 131I-EGFR-BSA-PCL. The animals injected with 131I-EGFR-BSA-PCL and 131I-BSA-PCL showed more uniform focused liposome distribution of the tumor area.
**Conclusion**: The results of this study demonstrated that EGFR-BSA-PCL and BSA-PCL had superior cellular binding and higher cellular uptake compared with the control 131I in vitro and in vivo, as demonstrated by the tumor size, body weight, histopathology, and SPECT images. With the use of novel therapeutic agents, the data presented in this study open new avenues in the treatment of colorectal cancer.

P_100

## Primary Hyperparathyroidism due to Functional Parathyroid Cysts: A Case Report and Literature Review

Yan-hui Ji, Jian Tan*, Gui-zhi Zhang, Wei Li, Feng Dong, Ya-jing He, Ren-fei Wang, Wei Zheng, Qiang Jia, Fu-hai Zhang
*Department of Nuclear Medicine, Tianjin Medical University General Hospital, China*

Parathyroid cysts (PCs) are rare and are often mistaken in the differential diagnosis of neck lumps. Most PCs are found to be non-functional, but those found to be functional are said to be caused by the cystic degeneration of parathyroid adenomas. We reported a case of a functional PC in a woman with clinical and biochemical features of primary hyperparathyroidism (PHPT). Laboratory investigation revealed increased serum calcium and parathyroid hormone (PTH) levels. The PTH level in the cyst was >263.0 pmol/L. A large cystic lesion was also observed during the neck ultrasonography and comuted tomography performed as a routine workup for PHPT. The lesion was first described as a cystic thyroid nodule. Tc99m sestamibi scintigraphy was performed to determine the existence of any parathyroid lesions; however, no radioactive uptake was observed. The serum PTH level decreased >50% postoperatively, and the result of the histopathological evaluation was consistent with an encapsulated parathyroid adenoma with a cystic center. In sum, we report a functional PC in a patient. PCs are among the rare causes of PHPT. The cystic adenomas of parathyroid glands are often misdiagnosed as thyroid cysts. PCs may be functioning or nonfunctioning and lack characteristic clinical or radiological features. PCs can be diagnosed on the basis of imaging and laboratory findings. FNA and PTH levels represent a valuable diagnostic tool and should be performed in all cystic neck swellings, especially when the diagnosis is in doubt. A surgical method of treatment is preferred for functional cysts. Cure was achieved in our patient after surgical excision with the PC.

P_101

## Multiple Factor Analysis on Achieving Disease-free Status by the First Radioactive Iodine Therapy on Post-operative Patients with Differentiated Thyroid Cancer

Liu Na, Zhang Guizhi, Jia Qiang, Tan Jian, Meng Zhaowei*
*Department of Nuclear Medicine, Tianjin Medical University General Hospital , Tianjin 300052, China*

Radioactive iodine (131I) therapy is essential for the management of patients with differentiated thyroid cancers (DTC). Unsuccessful 131I ablation drastically affects prognosis of these patients. This study aimed to analyze potential predictive factors influencing the achievement of a disease-free status by the first 131I therapy. This retrospective review included 315 DTC patients, and multiple factors were analyzed. Tumor size, pathological tumor stage, lymph node (LN) metastasis, distant metastasis, American Thyroid Association (ATA) recommended risks, pre-ablation thyroglobulin (Tg) and thyroid stimulating hormone (TSH) displayed significant differences between unsuccessful and successful group. Cutoff values of Tg and TSH to predict a successful outcome were 3.525 ng/mL and 99.700 uIU/ml by receiver operating characteristic curves analysis. From binary logistic regression, tumor stage T3 or T4, LN metastasis to N1b station, intermediate and high risks, pre-ablation Tg ≥ 3.525 ng/ml and TSH < 99.700 μIU/mL were significantly associated with unsuccessful outcomes. Logistic regression equation for achieving a disease-free status could be rendered as: y (successful treatment) = -0.270 - 0.503X1 (LN metastasis) - 0.236 X2 (Tg) + 0.015 X3 (TSH). This study demonstrated LN metastasis, pre-ablation Tg and TSH were the most powerful predictors for achieving a disease-free status by the first 131I therapy.

P_102

## An Improved Method for Establishment of Graves' Disease Model in BALB/c Mice

Wei ZHENG, Renfei WANG, Jian TAN, Ning LI, Zhaowei MENG
*Department of Nuclear Medicine, Tianjin Medical University General Hospital, China*

**Objective**: To build the stable Graves' disease (GD) BALB/c mice model by immunization and electroporation (EP).
**Methods**: Ninety mice were divided into 3 groups: experimental group (n=50), control group (n=20), blank group (n=20). Recombinant plasmid pcDNA3.1/TSHR268 was constructed and injected to bilateral gastrocnemius of experimental group mice on the first, fourth, seventh and tenth week. The same volume of normal saline was injected to the control group and blank group at the same time. Both experimental group and control group were subjected to EP at the same time and the same location to enhance immunization. The level of total serum thyroxin (T4) was tested by radioimmunoassay (RIA). The level of serum thyroid stimulating hormone (TSH) was tested by immunoradiometric assay (IRMA). The level of serum thyroid stimulating hormone receptor N-terminal (TRAb N) antibody and thyroid stimulating hormone receptor C-terminal (TRAb C) antibody were tested by ELISA. Whole body 99mTcO4- imaging was performed. The weight of all the mice and thyroid morphology and pathology were analyzed.
**Results**: GD BALB/c mice model was built successfully by injecting recombinant plasmid pcDNA3.1/TSHR268 and EP at the same time and on the same location to enhance immunization, the positive rate was 79.17% (38/48). Serum total T4 level increased from (12.05±4.23) ng/ml at the basic level to (52.51±23.58) ng/ml on the 12th week ($P<0.05$). TSH level decreased from (5.53±2.78) μIU/mL at the basic level to (1.43±0.89) μIU/mL on the 12th week ($P<0.05$). TRAb N antibody level increased from (0.006±0.002) mIU/ml at the basic level to (0.278±0.106) mIU/ml on the 12th week ($P<0.05$). And the TRAb C antibody level increased from (11.111±2.808) arbitrary unit (AU)/ml at the basic level to (46.701±26.436) AU/ml on the 12th week ($P<0.05$). On the 21st week the TSH was still on the lower level than preimmune ($P<0.05$). Although the T4, TRAb N and TRAb C decreased respectively, they were still on the higher levels than preimmune (all $P<0.05$). There were no obvious variation in control group and blank group. After 4 times immunizations, the ability of 99mTcO4- uptake of immunized mice's thyroid increased significantly. The mean weight of the experimental mice was lower than both control and blank groups ($P<0.05$). There were morphological changes of the thyroid glands of immunized mice, which were enlarged. Microscope examination of the thyroid tissues revealed that there were lymphocytes infiltration, less colloid and height of the epithelial cells increasing in experimental mice.
**Conclusion**: By injecting recombinant plasmid pcDNA3.1/TSHR268 and EP, GD mice model was successfully established.

SUPPORTING FUNDS: National Natural Science Foundation of China (Fund No. 81501510).

P_103

## Harmonic Versus LigaSure Hemostasis Technique in Thyroid Surgery: A Meta-analysis

Arun Upadhyaya[1], Tianpeng Hu[1], Zhaowei Meng[1], Xue Li[1], Xianghui He[2], Weijun Tian[2], Qiang Jia[1] and Jian Tan[1]
*Departments of [1]Nuclear Medicine and [2]General Surgery, Tianjin Medical University General Hospital, Heping, Tianjin 300052, P.R. China*

**Objective**: Energized vessel-sealing systems (Harmonic scalpel and Ligasure vessel sealing systems) have been proposed to save operation time and reduce post-operative complications. The aim of the present meta-analysis was to compare operation time, post-operative complications and other parameters between them in open thyroidectomy.
**Methods**: A systematic literature search (MEDLINE, Cochrane Library, EMBASE and ISI Web of Science) was performed to identify randomized controlled trials (RCTs) comparing Harmonic scalpel and Ligasure during open thyroidectomy until December 2015. After data extraction, statistics were performed by Review Manager 5.3 software.
**Results**: Twenty four publications were evaluated for eligibility, and 7 RCTs (981 patients) were included. The Harmonic scalpel significantly reduced surgical time compared with Ligasure techniques (8.79 minutes, 95% confidence interval, [-15.91, -1.67]; $P = 0.02$). The intra-operative blood loss, post-operative blood loss, duration of hospital stay, thyroid weight, and serum calcium level postoperatively did not significantly differ in the either group.
**Conclusion**: This meta-analysis showed superiority of Harmonic Scalpel only in terms of surgical time compared with Ligasure hemostasis techniques in open thyroid surgery.

## The Research on the Effects of Salivary Gland Function after Fixed Dose(100mCi) 131I Treatment of Differentiated Thyroid Cancer Patients

Lu Yanqi, Mu Xingyu, Fu Wei*
*Department of Nuclear Medicine, Affiliated Hospital of Guilin Medical University, China*

**Objective**: Discuss using a fixed dose(100mCi) of 131I treatment of differentiated thyroid cancer patients will cause damage to the salivary gland function.
**Methods**: In May 2015 to May 2016 in our department were 40 patients received 131I treatment of differentiated thyroid cancer patients before and after treatment the salivary glands of 99TcmO4- dynamic imaging were compared, Analysis before and after treatment in patients with salivary glands (parotid and submandibular gland) uptakeratio(UR) and sheddingratio(SR) function changes. Using SPSS 18.0 statistical software for data analysis, Measurement data with mean±standard deviation(x±s) said, comparison between group by t test, $P < 0.05$ for the difference was statistically significant.
**Results**: Parotid gland function of DTC patients before treatment: UR:L(22.9±2.6) R(24.5±2.7),SR:L(58.3±6.2) R(60.7±7.1) ; Parotid gland function of DTC patients after treatment: UR:L(20.7±1.9) R(22.2±2.3),SR:L(57.0±7.6) R(58.1±7.1). Submandibular gland function of DTC patients before treatment: UR:L(23.5±2.2) R(23.6±2.8),SR:L(56.2±7.4) R(62.0±7.3); Submandibular gland function of DTC patients after treatment: UR:L(21.2±2.3) R(24.3±1.8),SR:L(57.1±6.7) R(58.8±6.4).
**Conclusion**: Use fixed dose (100mCi) 131I treatment of differentiated thyroid cancer patients, salivary gland function in patients with no obvious damage.



## Analysis of Influential Factors for the Therapeutical Outcome of the First 131I Radiotherapy for Papillary Thyroid Carcinoma after Total Thyroidectomy

Chunlei Zhao, Jinyan Chen, Shengwei Fang, Peipei Zhang, Suyang Han, Gang Yu, Qiaojun Chen, Jie Chen
*Department of Nuclear Medicine, Hangzhou First People's Hospital Group, Hangzhou Cancer Hospital, China*

**Objectives**: To investigate the influential factors for the outcome of the first 131I therapy for papillary thyroid carcinoma (PTC) after total thyroidectomy.
**Methods**: One hundred and fifty-nine patients (45 males, 114 females, 43.4±12.2y old) with PTC after total thyroidectomy who underwent 131I therapy were retrospectively analyzed. Therapeutic outcome (1=uncure, 0=cure) was determined according to TSH stimulated Tg (sTg) , diagnostic 131I whole body scan (WBS) and other imaging modalities after 6 months. Twelve possible factors affecting therapeutic outcome including patients' age, gender, time interval between thyroidectomy and 131I therapy, primary tumors size and extrathyroidal extention, number and range of primary tumor lesions, lymph node metastases, thyroid remnant, pre-treatment TSH, sTg, TgAb, 131I therapeutic dose, result of Rx-WBS and SPECT after 131I therapy were analyzed using univariate and multivariate logistic regression. The ROC curves and diagnostic critical point (DCP) were analyzed to evaluate the predictive value of quantitative ones in the influential factors.
**Results and Conclusions**: The rate of cure of the first 131I therapy was 64.2% (102/159). Univariate and multivariate logistic regression analysis showed that lymph node metastases and sTg were influential factors. Taking sTg as a predictive factor for the outcome of 131I therapy, area under the ROC curve for sTg was 0.926 (95% CI : 0.888 ~ 0.963). The cut-off value of DCP of sTg was 2.97ng/ml with a sensitivity of 94.74% and specificity of 76.47%. PTC patients after total thyroidectomy with low sTg levels and few lymph node metastases are more likely cured in the first 131I therapy.

P_106

## Re-188 Effectively Enhance the Inhibiting Effect of Bevacizumab for Non-small Cell Lung Cancer

Jie Xiao[1,2], Xiao Li[1,2], Yanli Li[1,2], Hongcheng Shi[1,2], Dengfeng Cheng[1,2]*
[1]*Department of Nuclear Medicine, Zhongshan Hospital, Fudan University, Shanghai, China*
[2]*Shanghai Institute of Medical Imaging, Shanghai, China*

**Objectives**: Bevacizumab (Bev) has been proved its efficiency in retarding the neovascularization of tumor. To improve inhibiting effect and lower the dose with less toxicity of Bev in non-small-cell lung cancer (NSCLC), in this investigation, we utilized Re-188, which is one of β emitting radionuclides, labeled with Bev for radioimmunotherapy and imaging in nude mice bearing xenografeted A549 lung adenocarcinoma.
**Methods**: Re-188 was labeled with Bev using glucohepatonate as transchelator. Radio-TLC using 0.9% Nacl and mixed solution, (Vethanol: Vammonia: Vwater=2:5:1) was used to measure labeling rate and labeling stability of 188Re-Bev. After A549 cell were treated with bev alone, 188ReO4- alone and 188Re-bev at different concentration for 4 hours and 24 hours, CCK8 assay was carried out to determine viability of cells based on the OD values at 450nm in vitro. Flow cytometry was performed to detect the percentage of apoptosis in treated group, untreated group as control. NSCLC tumor models (n=20) were prepared and divided into four groups including control group, bev group, low-dose 188Re-bev group and high-does 188Re-bev group. The therapeutic response was determined by the alteration of tumor size, body weight, white blood cell account and 99mTc-MAG3-Bev.
**Results**: The labeling efficiency of Re-188-Bev was more than 97 %. After incubation with normal saline and mice serum for 24 hours, no obvious de-labeling was observed in vitro. CCK8 assay demonstrated that Re-188-bev exhibited markedly cytotoxic effects in time-dependent and radioactivity does-dependent manner compared with any other group (Two-way ANOVA, P value < 0.0001). The percentage of apoptosis cells measured by flow cytometry was consistent with CCK8 results. For tumor models, body weights were not significantly influenced by the introduction of Re-188-bev (11.1 MBq) What's more, the growth of tumor volumes was delayed after treatment with Re-188-bev two weeks later.
**Conclusions**: 188Re-bev, as a promising radio-therapeutic agent, can enhanced the therapeutic effect and reduced the side-effects of bev for NSCLC.

P_107

## Gender Impact on the Relationship between Thyroid Function and Serum Lipids in Patients with Differentiated Thyroid Cancer

Xue Li, Zhaowei Meng*, Jian Tan, Jianping Zhang, Qiang Jia
*Department of Nuclear Medicine, Tianjin Medical University General Hospital, Tianjin 300052, China*

**Objective**: We aimed to explore the association between thyroid stimulating hormone (TSH) and serum lipids in differentiated thyroid cancer (DTC) patients, emphasizing the risk of hyperlipidemia between different genders.
**Methods**: The study included 352 DTC patients who were ready to receive 131I therapy as well as 352 matched normal controls. In DTC group, 157 patients were monitored for TSH and lipid parameters before and after one-month of thyroxine therapy. T-test, Pearson bivariate correlation and binary logistic regression were performed. All participants were divided into 3 subgroups according to TSH levels, subgroup 1 (normal TSH level), subgroup 2 (TSH between 5 and 30 μIU/mL), and subgroup 3 (TSH higher than 30 μIU/mL).
**Results**: Serum total cholesterol (TC), triglycerides (TG), and low-density lipoprotein-cholesterol (LDL-C) levels were significantly higher in DTC group than in control group. Levels of these parameters decreased after thyroxine therapy. We observed significant positive correlations between TSH and TC, TG and LDL-C in both genders. Binary logistic regression showed female DTC patients had higher risks to develop hyperlipidemia than male patients. And the risks increased when TSH increased. For example, the risks of high TC in subgroup 2 were 3.30 in male and 4.60 in female, respectively. However, in subgroup 3, the risks were 9.40 in male and 13.12 in female, respectively.
**Conclusion**: Our results showed that after thyroidectomy, the danger for dyslipidemia increased obviously in DTC patients. More importantly, female patients had higher risk than male patients.

P_108

## The Effect of L-thyroxine Treatment Versus Placebo on Serum Lipid Levels in Subclinical Hypothyroidism

Xue Li, Zhaowei Meng*, Qiang Jia ,Guizhi Zhang, Jian Tan
*Department of Nuclear Medicine, Tianjin Medical University General Hospital, Tianjin 300052 China*

**Objective**: Subclinical hypothyroidism is a common disease. But whether L-thyroxine replacement treatment can affect serum lipids in subclinical hypothyroidism is still controversial. The object of this meta-analysis is to assess the effect of L-thyroxine therapy on serum lipid levels in subclinical hypothyroidism.
**Patients and methods**: Sources were retrieved from the Cochrane Library, PubMed, Medline, Google Scholar, and Embase until July 2015. We selected all randomized controlled trials (RCTs) about the effects of L-thyroxine replacement on serum lipid levels. After screening, eligible RCTs were included in our meta-analysis. Statistics were performed by Review Manager 5.2 software. All the assessed outcomes were continuous data.
**Results**: Seven RCTs involving 319 patients were included. The overall methodological quality of the RCTs was good. After statistical analysis, we found serum low density lipoprotein-cholesterol (LDL-C) level was decreased significantly after L-thyroxine treatment (mean difference [MD] -0.23; 95% confidence interval [CI]: [-0.44,-0.03]; P=0.02). Whereas the changes of total cholesterol (TC), triglyceride (TG) and high density lipoprotein-cholesterol (HDL-C) were not significant (MD -0.18, P=0.09; MD -0.02, P=0.78; and MD -0.06, P=0.14; respectively).
**Conclusion**: By summarizing all available RCTs evidence about the effect of L-thyroxine on serum lipid levels in subclinical hypothyroidism, we found significant improvement of serum LDL-C levels, however, serum TC, TG and HDL-C levels showed no change.

P_109

## Study on the 99Tcm-TP1623 and Evaluate Its Targeting Properties in Vitro

Mengzhi Zhang, Yanxing Guan*
*Department of Nuclear Medicine, The First Affiliated Hospital Of Nanchang University, Nanchang 330006,China*

**Aim**: the goal of the study was to develop a method for 99Tcm labeling of TP1623(the human epidermal growth factor receptor 2-binding Affibody molecule) using the GAGG chelator, which was incorporated into TP1623 using peptide synthesis,and evaluate the targeting properties of the labelled conjugate in vitro.
**Methods**: The Affibody molecule TP1623 was synthesized by solid phase synthesis, and the N-terminal coupled GAGG chelator, while the C-terminal amidation though NH2;Then the products was lablled with99Tcm.labelling rate and radiochemical purity was analyse by paper chromatography and high performance liquid chromatography. stability in vitro of the compound was perform at 0h、2h、4h、6h after lablled. And perform the largest combined radioactivity experimental of TP1623.The HER2-overexpress human breast cancer cell SKBR3 was detect by cell immunohistochemistry. In vitro binding of the resulting radioconjugate was characterized by receptor saturation and competition assays.
**Results**: The molecular probe was successfully synthesized and lablled with 99Tcm with the labeling rate of 96.5%,The radiolabelled molecular remained highly stable in vitro. Until 6h,the labelling rate still 93.2%. The radiochemical purity was 93% by HPLC. And the max combined radioactivity was 1110MBq,its labelling rate over 90%. The cell immunohistochemistry has proved that SKBR3 cell membrane positive result(++++),the whole membrane was in brown. The saturation and competition curve mean labelled affibody molecule still in accordance with the basic characteristic of nonlabel affibody molecule, no negative influence after labelled .And it also indicated that it has a high-affinity binding to HER2.In addition, by competition assays provided evidence it was through HER2 –mediated binding to the HER2-expressing cell.
**Conclusion**: The 99Tcm-TP1623 molecular probe is a promising tracer agent, and the results in this study provide a foundation for further study in imaging of breast cancer tumor- burdened mice, even for earlier visual detection of HER2-positive cancer in the clinical in future.

P_110

## Influence of Chelator and Near-infrared Dye Labeling on Biological Properties of Dual-labeled Trastuzumab-based Imaging Agents

Xuejuan Wang[1]*, Melissa B. Aldrich[2], Zhi Yang[1], Nina Zhou[1], Qing Xie[1], Chen Liu[1], Eva Sevick-Muraca[2]
[1] *Key laboratory of Carcinogenesis and Translational Research (Ministry of Education), Department of Nuclear Medicine, Peking University Cancer Hospital & Institute, Beijing 100142,China*
[2] *Center for Molecular Imaging, the Brown Foundation Institute of Molecular Medicine, University of Texas Health Science Center at Houston, Houston, Texas*

**Objective**: To investigate the effect of fluorescent dye labeling on the targeting capabilities of 111In-(DTPA)n-trastuzumab-(IRDye800)m.
**Methods**: Trastuzumab-based conjugates were synthesized and conjugated with diethylenetriaminepentaacetic acid (DTPA) at molar ratios of 1, 2, 3, and 5 and with a fluorescent dye (IRDye800 CW) at molar ratios of 1, 3, and 5. Immunoreactivity and internalization were assessed on SKBR3 cells, overexpressing human epidermal growth factor receptor 2. The stability in human serum and phosphate buffer saline (PBS) was evaluated. The biodistribution of dual-labeled conjugates were compared with that of 111In-(DTPA)2-trastuzumab in a SKBR3 xenograft model to evaluate the effect of dye-to-protein ratio.
**Results**: All trastuzumab-based conjugates exhibited a high level of chemical and optical purity. Flow cytometry results show that increasing dye-to-protein ratios were associated with decreased immunoreactivity. Stability studies revealed that the conjugate was stable in PBS, while in human serum, increased degradation and protein precipitation was observed with increasing dye-to-protein ratios. At 4 h, the percentage internalization of dual-labeled conjugates normalized by dye-to-protein ratio (m) were 24.88 ± 2.10%, 19.99 ± 0.59%, and 17.47 ± 1.26% for “m” equal to 1, 3, and 5, respectively. A biodistribution study revealed a progressive decrease in tumor uptake with an increase in the dye-to-protein ratios. The liver, spleen, and kidneys showed a marked uptake with increased dye-to-protein ratios, particularly in the latter.
**Conclusion**: With non-specific-site conjugation of the fluorescent dye with a protein based imaging agent, the increase in dye-to-protein ratios negatively impacted the immunoreactivity and stability, indicating a reduced tumor uptake.

P_111

## Preclinical Characterization of Positron Nuclide and Near Infrared Dye Dual-labeled Trastuzumab Fab Fragment in HER2 Positive Breast Cancer

Xuejuan Wang[1,2], Melissa B. Aldrich[2], Yan Zhang[1], Nina Zhou[1], Qing Xie[1], Chen Liu[1], Zhi Yang[1], Eva Sevick-Muraca[2]
[1] *Key laboratory of Carcinogenesis and Translational Research (Ministry of Education), Department of Nuclear Medicine, Peking University Cancer Hospital & Institute,Beijing 100142, China*
[2] *Division of Molecular Imaging, the Brown Foundation Institute of Molecular Medicine, University of Texas Health Science Center at Houston, Houston, Texas, USA 77030*

**Purpose**: By dual labeling a targeting moiety with both positron and optical probes, the ability for noninvasive imaging and intraoperative guidance may be possible. Our objective was to synthesize a dual-labeled trastuzumab Fab fragment-based imaging agent that can be used in identifying lesions of HER2-positive breast cancer via positron emission tomography (PET) and near-infrared (NIR) fluorescence imaging.
**Methods**: Trastuzumab Fab fragment were generated from trastuzumab by using digesting enzyme papain. 64Cu-DOTA-trastuzumab Fab-IRDye800 was synthesized by a standard three-step procedure. Purity, stability, immunoreactivity, and targeting property were explored. MicroPET and NIR fluorescence scans was carried out in a HER2-positive breast cancer SKBR-3 xenograft model.
**Results**: 64Cu-DOTA- trastuzumab Fab-IRDye800 was demonstrated high purity by both chemical and fluorometric determinations. The dual-labeled conjugate was stable in PBS, but not in serum after 48 h at 37° C. Larger molecules (> 80KD) were seen after a 48-h incubation in human serum. Both flow cytometry and the Lindmo assay demonstrated a specific binding affinity of dual-labeled tracer to HER2- overexpressing SKBR-3 cells. Primary tumors were visualized with 64Cu-DOTA- trastuzumab Fab-IRDye800 via MicroPET and NIR fluorescence. Liver and kidney showed uptake of the dual-labeled imaging agent.
**Conclusion**: 64Cu- DOTA-trastuzumab Fab-IRDye800 may be an effective specific diagnostic imaging agent for locating HER2-positive breast cancer lesions via multimodality imaging.

P_112

## Anti-migratory Effectof Rapamycin Impairs Allograft Imaging by 18F-fluorodeoxyglucose-labeled Splenocytes

Hukui Sun[1], Huaiquan Wang[1], Ting Liang[2], Guihua Hou[2]
[1] *Nuclear Medicine Department, Central Hospital of Zibo, Shandong University, Zibo, Shandong, China*
[2] *Institute of Experimental Nuclear Medicine, School of Medicine, Shandong University, Jinan, Shandong, China*

**Objective(s)**: Tracking lymphocyte migration is an emerging strategy for allografts imaging. In the present study, the feasibility of using rapamycin-treated 18F-fluorodeoxyglucose (18F-FDG)-labeled splenocytes for the in vivo imaging of allografts was evaluated.
**Methods**: BALB/c 18F-FDG-labeled splenocytes with or without rapamycin pretreatment (designated as FR and FC cells, respectively) were transferred into recipient mice 30 days later. Imaging of radiolabeled cells in the skin grafts was conducted through in vivo dynamic whole-body phosphor-autoradiography and histological analysis.
**Results**: Whole-body phosphor-autoradiography revealed reduced radioactivity in allografts of mice received FR cells compared with those received FC cells, at 30, 60 and 90 min. The peak of allograft to opposite native skin ratio (AOR) was significantly lower in the FR cell group (1.29±0.02 at 60 min) compared with the FC cell group (3.29±0.17 at 30 min; P<0.001). A significant accumulation of FC cells in allografts was detected at 30 min following injection, however, images of FR cells did not enable graft visualization at any time point. The radioactivity of the allografts was observed to be correlated with the transferred cells, which were observed histologically (r2=0.887;P<0.001).
**Conclusion**: Our results suggest that splenocyte trafficking was impaired by the mTOR inhibitor, imaging of these cells may not be possible in the presence of rapamycin.

P_113

## The Combined Impacts of Blood Glucose Level and Glucose Metabolism Related-factors on Liver FDG Uptake

Hu Yan[1,2,3], Liu Guobing[1,2,3], Li Yanli[1,2,3], Shi Hongcheng[1,2,3]
[1] *Shanghai Institute of Medical Imaging, China*
[2] *Department of Nuclear Medicine, Zhongshan Hospital, Fudan University, China*
[3] *Institute of Nuclear Medicine, Fudan University, China*

**Objectives**: To evaluate the combined impacts of blood glucose and its related metabolic factors on 18F-FDG uptake by liver.
**Methods**: A total of 544 healthy subjects (384 male and 160 female, age from 24 to 73) with 18F-FDG PET/CT were recruited for analysis. Mean standard uptake value (SUVmean) in the right lobe of liver was calculated. Independent-sample T test and One-way analysis of variance were performed to compare SUVmean between genders and body mass index (BMI) levels, Correlation, partial correlation analysis and multiple linear regression analysis were conducted to evaluate the relationship between age, injected 18F-FDG dose, blood glucose, serum T3, T4, FT3, FT4, basic metabolic rate (BMR), BMI and liver SUVmean.
**Results**: The SUVmean of the liver was 1.90 ± 0.409 with no statistic difference between genders (t=0.693, P=0.489) but with significant discrepancy among BMI groups (F=3.056, P=0.028). Age, blood glucose and FT3 were significantly associated with liver SUVmean (partial correlation coefficient r'=0.108, 0.140 and 0.016 respetively, with P all <0.05) and were independent factors that indicated variation of liver SUVmean (β coefficient =0.006, 0.007 and 0.080, P all <0.05), of which blood glucose owns the strongest power predicting variation of liver SUVmean (standardized β coefficient=0.154, P<0.001).
**Conclusions**: Blood glucose and its related metabolic factors affect the liver 18F-FDG uptake. Age, FT3, blood glucose are independent factors predicting variation of liver SUVmean. The impact of glucose metabolism status should be considered when assessing liver 18F-FDG uptake, clinically.

P_114

## Role of 18F-FDG PET/CT in Staging and Restaging of Cutaneous Melanoma

Yan Fan, Jianhua Zhang, Zhenghao Tong, Lijuan Di, Rongfu Wang
*Nuclear Medicine Department of Peking University First Hospital, Beijing, China*

**Objective**: To investigate the role of 18F-FDG PET/CT in staging and restaging of cutaneous melanoma.
**Methods**: Forty-eight patients (17 patients for staging and 31 patients for restaging) with cutaneous melanomaunderwent 18F-FDG PET/CT between Sep 2013 and Oct 2015 were retrospectively analyzed. Primary melanoma lesions and metastatic lymphnodes were confirmed by pathology.
**Results**: Of all the 48 patients, the distribution of primary cutaneous melanoma in order of frequency were foot (n=18), hand (n=12), scalp (n=3), back (n=3), thigh (n=3), face (n=2), vulva (n=2), axilla (n=2), hip (n=1), umbilicalregion (n=1) and upper arm (n=1). In 17 patients for staging, SUVmax of the primary melanoma sites ranged from 0 to 7.2. Based on the results of pathology, 11 patients were with lymphnode metastasis and 1 patient was with both lymphnode and lung metastasis. In 11 (91.6%) of 12 patients with metastasis, PET/CT detected sites of abnormal 18F-FDG uptake having the SUVmax ranged from 0.8 to 9.5. In 1 patient with umbilical melanoma, left axillary lymphnode metastasis was not detected by PET/CT. Three patients had false-positive PET/CT findings, inflammation of lymphnodes were diagnosed. For the specific diagnosis of staging and restaging of cutaneous melanoma, PET/CT had overall sensitivity, specificity, and accuracy of 91.6%, 92.3%, and 91.6%, respectively.
**Conclusion**: According to the preliminary data,18F-FDG PET/CT is of great importance for staging and restaging of cutaneous melanoma.

P_115

## The Influence of the Kidney Depth Correction of Renal Dynamic Imaging Measurement of GFR Values

Lu Yanqi, Fu Wei*
*Department of Nuclear Medicine, Affiliated Hospital of Guilin Medical University, China*

**Objective**: A compare with the GFR values between renal dynamic imaging and using ultrasound to correction the kidney depth measure before dynamic renal imaging based on the different height and weight of patients, to assess the effect of depth correction of GFR values in renal dynamic imaging.
**Methods**: (1) A retrospective analysis of 73 cases from 11/2015 to 2/2016,40 males and 33 females, aged 20 to 29 in 2 cases,6 cases of 30~39,12 cases of 40~49,25 cases of 50~59,19 cases 60~69,9 cases more than 70 years old;(2) Ultrasound measurement of bilateral renal hilum to the back surface vertical distance of the skin(cm); calculate the left and right kidney depth (cm);(3) Renal dynamic imaging with 99mTc - DTPA, Input the height (cm) and weight (kg) of patients in the image processing, outline the kidney ROI, along the outer renal cortex and sketch a closed curve, including the renal pelvis and calyces, background ROI, on the edge of the kidney from the lateral cortex of 2 ~ 4 pixels, sketch about 40 ~ 70 pixel size crescent background, with classic Gates analysis method to determine the double kidney GFR,(4) Will be adjusted renal dynamic data into the original formula to measure GFR(Don't change the kidneys and background ROI).
**Results**: Gates to measure 73 patients of left, right and total kidney GFR values, respectively (39.28±5.34), (37.26±5.43), (76.55±7.51)ml/min, While after depth correction of GFR values, respectively (47.55±4.61), (44.85±4.39) and (92.40±6.47)ml/min, The differences were statistically significant ($P<0.05$).
**Conclusion**: Many factors that affect the determination of GFR of renal dynamic imaging, the kidney depth is an important influencing factors, using ultrasound in depth correction is a kind of simple method to individualized attenuation correction on the depth of the kidney. Applied to the Gates method can improve the accuracy of the determination of GFR, especially the height, weight and kidney angle was abnormal, so as not to cause kidney GFR dynamic measurement error.

## Comparison of 18F-FCH and 18F-FDG PET / CT Dual Tracer Imaging in the Grading of Cerebral Gliomas

Wen Xin, Li Yan-peng, Cheng Bing, Xie Xin-li, Wang Rui-hua, Han Xing-min*
*Department of Nuclear Medicine,The First Affiliated Hospital of Zhengzhou University, China*

**Objective**: To compare the value of the gliomas grading by 18F-FDG and 18F-FCH PET/CT, in order to provide more reliable information for the clinical treatment.
**Materials and Methods**: Thirty-three patients with suspected brain gliomas underwent 18F-FDG PET/CT examination, 31 of them underwent dual-phase 18F-FCH PET/CT imaging in the next day, acquisition time were 10 minutes and 40 minutes respectively after injection. All images analyzed by visual and semi-quantitative (SUVmax and the lesion to the contralateral white matter ratio, L/WM). All cases have the immunohistochemistry and pathology information. Compare PET/CT findings of two tracers with the grade of gliomas. Statistical analysis using SPSS 21.0, P <0.05 was considered statistically significant.
**Result**: Visual analysis: distinction between high-grade from low-grade gliomas, 18F-FDG and 18F-FCH sensitivity are as follows: 89.47% and 100%, specificity of 88.89% and 88.89%, accuracy of 89.28% and 96.30%. Semi-quantitative analysis: ①SUVmax of FDG vs FCH: Grade II 4.25±1.11 vs 0.33±0.17, Grade III 9.49±2.89 vs 2.40±0.88, Grade IV 10.05±4.57 vs 3.46±0.89, all P <0.05. ②L/WM of FDG vs FCH: Grade II 0.95±0.20 vs 1.27±0.48, P=0.071; Grade III 1.86±0.44 vs 6.97±2.82, P <0.05; Grade IV 2.19±0.95 vs 10.96±2.26, P <0.05. ③The concentration of both tracers in gliomas correlated with tumor grade and Ki-67 index. ④SUVmaxFCH of normal vs delay: Grade II 0.33±0.17 vs 0.33±0.08, P=1.0; Grade III 2.39±0.88 vs 2.89±1.98, P =0.263; Grade IV 3.47±0.89 vs 3.87±1.13, P=0.013; ⑤ L/WMFCH: normal vs delay, Grade II 1.27±0.48 vs 1.32±0.40; Grade III 6.97±2.82 vs 9.62±8.75; Grade IV 10.92±2.26 vs12.41±3.89, all P>0.05.
**Conclusion**: Both tracers can distinguish high-grade from low-grade gliomas. The concentration of both tracers in gliomas correlated with tumor grade and Ki-67 index. The uptake of 18F-FCH in delay phase was higher in high-grade gliomas than normal phase, particularly in grade IV; the increased concentration of 18F-FCH in delayed phase considered as a high degree of malignancy.



## Inflammatory SPECT/CT Imaging Based on 99mTc Labelled Anti-CD11b Antibody Allows Detecting Vulnerable Plaques and Assessing Therapeutic Effects of Atorvastatin to Atherosclerosis

Guobing Liu[1,2,3], Xiao Li[1,2,3], Yan Hu[1,2,3],Jie Xiao[1,2,3], Yanli Li[1,2,3], Yanzhao Zhao[1,2,3], Dengfeng Cheng[1,2,3]*, Hongcheng Shi[1,2,3]*
[1] *Department of Nuclear Medicine, Zhongshan Hospital, Fudan University, Shanghai, China.*
[2] *Institute of Nuclear Medicine, Fudan University, Shanghai, China*
[3] *Shanghai Institute of Medical Imaging, Shanghai, China*

**Objectives**: To investigate feasibility of 99mTc-anti-CD11b based SPECT/CT for detecting vulnerable plaques and assessing therapeutic effects of atorvastatin (AT).
**Methods**: 99mTc-MAG3-anti-CD11b was fabricated. ApoE-/- mice were fed with high-fat diet (HFD, group A), and C57 mice fed with chow diet (group B) for control; while in group C, ApoE-/- mice were fed with chow diet and AT (10mg/kg/day) to 20 weeks after 8w-HFD feeding. Mice weight, serum lipids, cytokines, circulating CD11b+ cells and CD11b expression were tested. SPECT/CT were performed to detect plaques and to evaluate therapeutic effects of AT. Aortic breast specific gamma imaging (BSGI), Oil-Red-O staining and CD-11b-IHC staining were performed to confirm SPECT/CT findings.
**Results**: Group-A mice showed higher serum lipids, cytokines, body weights, and CD11b+-cells with higher CD11b expression than group B and group C (P<0.05). Aortic Red Oil O staining showed higher plaque-area percent in mice of group A than group B (P<0.001) and group C (P=0.039). The plaque-to-background ratio (P/B) on SPECT/CT images were higher in mice of group A than group B and group C (P<0.05). The findings were consistent with aortic BSGI imaging, Oil-Red-O staining and IHC staining. Positive relation was identified between P/B ratio on SPECT/CT and CD11b-expression on IHC (r=0.696, P=0.017).
**Conclusion**: Anti-CD11b-Ab mediated SPECT/CT imaging is capable for identifying inflammatory vulnerable plaques and evaluating therapeutic effectiveness from AT.

P_118

## Longitudinal Changes in FDG PET SUVR in APOE ε4 Carriers and Non-carriers in Alzheimer's Disease Neuroimaging Initiative Study

Xueqi Chen[1], Haoyin Cao[2], Rongfu Wang [1]*, Yun Zhou [1,3]*
[1] *Department of Nuclear Medicine, Peking University First Hospital, Beijing, China*
[2] *University Hospital, Hamburg-Eppendorf, Hamburg, Germany*
[3] *The Russell H. Morgan Department of Radiology and Radiological Science, Johns Hopkins University School of Medicine, Baltimore, Maryland, United States of America*

**Objective**: Several biomarkers have been proved to be associated with the presence and progression of Alzheimer's disease (AD). However, the dynamic changes of FDG biomarkers in longitudinal study are not fully understood, partly because AD develops over many years. Although APOE ε4 is a major genetic risk marker in AD, the effect of APOE ε4 on the longitudinal changes of FDG is still under controversial discussion. The aim of our study is to assess the effect of APOE ε4 genotype on glucose metabolism measured by 18F-FDG PET.
**Methods**: We investigated 82 Alzheimer's Disease Neuroimaging Initiative (ADNI) subjects [48 MCI (Mild cognitive impairment group) (24 converted to AD) and 34 NC (Normal control group) (10 converted to MCI or AD)] for up to 96 months (median= 84 months). 18F-FDG PET scans were conducted at each follow-up time. All preprocessed 18F-FDG images were spatially normalized to MNI space using MRI and SPM8. 35 regions of interest (ROI) were manually drawing in a high resolution MRI template from VBM8. Standard uptake values ratios (SUVR) to cerebellum were calculated. All the subjects were divided into APOE ε4 carriers and non-carriers based on their APOE ε4 status. Region-based mixed linear model was used for the evaluation of APOE ε4 effect, with sex and age at baseline were included as covariates.
**Results**: The mixed linear model regression demonstrated that the rate of SUVR changes for parietal was accelerated ($p=0.0076$) in MCI group in the APOE ε4 carriers. Both parietal and caudate showed the different rate of SUVR changes in modified MCI group (selected baseline scan and last scan only) in APOE ε4 status. None of the regions in NC group and all FDG group (MCI+NC group) was significantly affected by APOE ε4 status. More regions were found significant in SUVR changes between APOE ε4 carriers and non-carriers in MCI group, NC group and all group, respectively, when FDG scans over 24 months visit were included in the analysis.
**Conclusion**: APOE ε4 affects the rate of changes of FDG SUVR in the longitudinal AD study, and 24 months may be a turning point for the trend of SUVR changes.

P_119

## Diagnosis and Differential Diagnosis of Multiple Myeloma in 18F-FDG PET/CT

Cao Dengmin
*Department of Nuclear Medicine, Fujian Provincial Hospital, Fuzhou City, China*

**Objective**: To analyse the imaging features of Multiple Myeloma (MM) in 18F-FDG PET/CT, and explore PET/CT value of diagnosis and identified diagnosis in MM.
**Methods**: A total of 24 patients with Multiple Myeloma confirmed by pathological histology in our hospital from September 2010 to March 2016 were analyzed retrospectively, and there are 15 males and 9 females, aged 45~73 years old, average age is 59.42±9.35 years old .
**Results**: We can see 23 cases of multiple bone destruction ( 95.83%), 16 cases of diffuse distribution (66.67%), 7 cases of scattered in the distribution (29.17%), 1 case of bone destruction without being obvious(4.17%). Besides, 14 cases with pathological fracture (58.33%), 11 cases with the soft tissue mass (45.83%), and 7 cases with osteogenic change (29.17%). Patients with newly diagnosed may have external organ invasion. Diffuse or multiple punctiform and osteolytic destruction were showed in PET/CT, and the whole body bone lesions of 18F-FDG uptake is not uniform, SUVmax is 5.41±3.47, the pathological fracture SUVmax is 4.10±2.17, the osteoblastic lesions SUVmax is 2.89±1.57, and the soft tissue mass SUVmax is 5.12±3.78. The destruction of bone and the hypermetabolism region may not be consistent.
**Conclusion**: PET/CT has high clinical application value in the diagnosis and differential diagnosis of MM from two aspects of metabolism and anatomy.

## Clinical Research of Radionuclide Imaging on Assessing Ventricular Systolic Synchrony and Ventricular Function in Patients with Chronic Heart Failure

Li Ting , Li Jianming
*TEDA International Cardiovascular Hospital, China*

**Objective**: To discuss some problems which related to cardiac systolic dyssynchrony in patients with chronic heart failure by GSMPI.
**Methods**: 41 healthy people, who composed of the normal control group, and 82 CHF patients were classified into grade I - IV four groups. Undertook GSMPI, acquired the functional parameters. Compare the difference of PHB, PSD, and LVEF between the CHF group and the control group separately; Compare the difference among the four CHF groups. Compare the difference of some clinical factors between the two groups; Analysis the incidence rate of mechanical dyssynchrony in the different heart function classifications; Discuss the relationship among the cardiac synchrony and myocardial perfusion.
**Results**: There's no obvious difference of PHB, PSD, between the NYHA I CHF patients and the control group; Significant different exited between the NYHA II –IV class and the control group. Significant different of PHB, PSD and LVEF among the 4 CHF groups. The incidence rate of DM, LVEF, EDV and SRS were significant different between the patients who with and without systolic dyssynchrony. PHB and PSD were both positively correlated obviously with SSS/SRS.
**Conclusion**: The systolic dyssynchrony degree increased accompanied by the heart failure progression; Diabetes mellitus, LVEF, EDV, ESV, SSS/SRS are influence factors of the systolic dyssynchrony; The increase of the extent of impaired myocardial blood flow will aggravate the cardiac systolic dyssynchrony. The GSMPI parameters can be used as the quantitative indicators for choosing the patients with early heart failure, guiding the clinical early diagnosis and treatment.



## Simultaneous SPECT Imaging of Multi-targets to Assist in Identifying Hepatic Lesions

Zhide Guo[1, 2], Mengna Gao[1], Deliang Zhang[1], Duo Xu[1], Guibing Chen[3], Xinhui Su[4], Pingguo Liu[4], Hua Wu[3], Jin Du[2], Xianzhong Zhang[1]*
*[1] Center for Molecular Imaging and Translational Medicine, State Key Laboratory of Molecular Vaccinology and Molecular Diagnostics, School of Public Health, Xiamen University, Xiang'an South Rd, Xiamen 361102, China;*
*[2] Department of Isotope, China Institute of Atomic Energy, P. O. Box 2108, Beijing 102413, China;*
*[3] The First Affiliated Hospital of Xiamen University, Zhenhai road, Xiamen 361103, China;*
*[4] Zhongshan Hospital Affiliated of Xiamen University, Hubin South Road, Xiamen 361004, China*

**Objectives**: Liver diseases exhibit complicated elements including lesion localization, acute and chronic inflammation, and changes in paracarcinomatous tissues. Usually the changes of involved receptors and microenvironment will directly affect the tumor progress and therapeutic efficacy. Molecular imaging technique is an attractive tool to detect liver disease at early stage. Here in this study, we tried to detect multiple targets simultaneously in one imaging operation to offer more biological information for disease diagnosis or therapy.
**Methods**: This study developed a simultaneous dual-isotope single photon emission computed tomography (SPECT)/CT imaging method to assist diagnosis of hepatic tumor and liver fibrosis. Before in vivo experiment, in vitro simulated imaging studies with 131I and 99mTc were performed to verify the feasibility and practicability. Then on the base of these, the in vivo imaging studies were performed using animal models. Animal models of liver fibrosis and orthotopic human hepatocellular carcinoma (HCC) were established and validated by ex vivo autoradiography, tissue analysis, PET/CT and MRI. Initial studies were performed in vitro to assess the feasibility for achieving dual-isotope imaging. The aforesaid star probes (131I-NGA and 99mTc-3P-RGD2) were adopted in this new developed imaging protocol to detect ASGPR and integrin receptors for better understanding of liver diseases. SPECT imaging and biodistribution study were carried out to verify the feasibility and superiority.
**Results**: As expected, 99mTc-3P-RGD2 had the ability to evaluate liver fibrosis and detect tumor lesions. 131I-NGA showed that it was effective in assessing the anatomy and function of the liver. The static pinhole SPECT images were acquired simultaneously at 30 min after injection of the mixture of 99mTc-3P-RGD2 and 131I-NGA. The tissue distribution derived from SPECT images of nor-mal mice, fibrotic mice and orthotopic liver tumorous mice, which obtained from 131I-NGA window using dual-isotope protocol, almost same as the 131I-NGA only imaging. High liver accumulations were found in normal mice and defect liver uptake in fibrotic mice, while no uptake of lesion site in orthotopic liver tumorous mice. The correlation between radioactivity uptake and ASGPR expression indicated that it is possible to quantify the ASGPR by using dual-isotope SPECT imaging protocol to eva-luate the hepatic function with 131I-NGA. From 99mTc window, significant uptake of 99mTc-3P-RGD2 were found in fibrotic liver due to increased expression of αvβ3 on hepatic stellate cell. High tumor and kidney activity accumulation was observed in LM3 tumorous mice at 30 min p.i.. Similarly, the tissue distribution pattern of 99mTc-3P-RGD2 obtained from dual-isotope protocol was almost the same as that with single 99mTc-3P-RGD2 tracer.
In order to further confirm the consistency of single and dual-isotope SPECT imaging, 99mTc-3P-RGD2 or 131I-NGA only was injected in mice bearing LM3 tumor xenografts and liver fibrosis for SPECT imaging, respectively. The images from dual-isotope protocol have been further analyzed and compared with single isotope protocol. The tissue distribution pattern of tracers in dual-isotope protocol was consistent well with that of single tracer. In single isotope imaging, the fibrosis-to-control ratios were about 0.80 (Fib-4 W) and 0.65 (Fib-8 W) for 131I-NGA, 1.65 (Fib-4 W) and 2.34 (Fib-8 W) for 99mTc-3P-RGD2, respectively. While, in dual-isotope imaging, the ratios were about 0.81 (Fib-4 W) and 0.70 (Fib-8 W) for 131I-NGA, 1.71 (Fib-4 W) and 2.56 (Fib-8 W) for 99mTc-3P-RGD2, respectively. In LM3 tumorous model, there is no significant difference between single isotope and dual-isotope imaging. The liver uptakes of 131I-NGA in tumor bearing mice were about 45.36 %ID/g (single isotope) and 48.18 %ID/g (dual-isotope), respectively. At the same time, the tumor uptakes of 99mTc-3P-RGD2 were about 9.03 %ID/g (single isotope) and 8.59 %ID/g (dual-isotope), respectively.
**Conclusion**: In summary, synchronized dual-isotope SPECT/CT imaging to assist in diagnosis of hepatic tumor and liver fibrosis is feasible, and will have great potential in clinic. This strategy offers many potential advantages: additional, valuable information content without anatomical misregistration and significantly shorten the scan time. Furthermore, this technique could reduce the burden on both patients and medical staffs. Dual-isotope imaging has the ability to extend the application of SPECT, and with the possibility for synchronized tri-, tetra-, or more targets imaging. Although the radiation exposure of additional isotopes is an issue worthy of concern, with the continued improvement in instrument sensitivity, injected-probe activities will be reduced and the increased exposure can be alleviated.

## Synthesis and Evaluation of 18F-labelled Estradiol Derivative as an Estrogen Receptor Probe

Duo Xu[1]; Rongqiang Zhuang[1]; Linyi You[1]; Zhide Guo[1,2]; Deliang Zhang[1]; Pu Zhang[1]; Hua Wu[3]; Xianzhong Zhang[1]*
[1] *Center for Molecular Imaging and Translational Medicine, State Key Laboratory of Molecular Vaccinology and Molecular Diagnostics, School of Public Health, Xiamen University, Xiang'an South Rd, Xiamen 361102, China;*
[2] *Department of Isotope, China Institute of Atomic Energy, P. O. Box 2108, Beijing 102413, China*
[3] *The First Affiliated Hospital of Xiamen University, Zhenhai Road, Xiamen 361003, China*

**Objective**: Breast cancer is a major female health problem in the world. We know that about 70–80% of breast carcinomas are estrogen receptor (ER) positive. Different receptor types and levels of breast cancer should be treated with different methods. With the development of positron emission tomography (PET), many estrogen derivatives had been labeled with 18F or other radioisotopes, making it possible to image the living condition with intuitive quantitation and reflect the change of estrogen receptor level. Among all of the ER+ imaging agents, 16α-18F-17β-estradiol (18F-FES) is the most successful one. 18F-FES has good affinity for the ER, which currently entered into the second phase of clinical experiment to predict response to first line hormone therapy in women with ER+ metastatic breast cancer. However, 18F-FES metabolized rapidly mainly through the liver, which leads to an increase of non-specific binding. Therefore, we designed a novel estradiol analog probe by adding a polyethylene glycol (PEG) to estradiol through "click" methods. PEG is a useful chain used to lower the lipophilicity of the whole molecular. The addition of the PEG decreased the liver metabolism and increased the probability of tumor uptake. The radiopharmaceutical was produced in high radiochemical purity and yield. We compared 18F-ETP with 18F-FES mainly in the following aspects: the octanol/water partition coefficient, uterus uptake and positron emission tomography (PET) imaging to prove 18F-ETP is an ideal ER imaging agent for breast cancer.
**Methods**: The 18F-ETP was radiolabelled with 18F using "click" methods. The in vitro stability of 18F-ETP was tested in serum and physiological saline, analyzed by High Performance Liquid Chromatography (HPLC). Radioactive peaks were monitored at different incubation time points. The octanol/water partition coefficient of 18F-ETP was measured in 1-octanol and deionized water according to a procedure published previously. MCF-7 (ER+) and MDA-MB-231 (ER-) cell lines were used to conduct cell uptake experiment. For the blocking study, MCF-7 cell line was treated with the ER inhibitor estradiol. To establish tumor-bearing animal models, both cell lines were implanted subcutaneously in Balb/c nude mice. After 18-30 days, mice were imaged after intravenous injection of 18F-ETP or 18F-FES (5.92 MBq/200 μL). To assess the specific targeting of tracer to ER, mice bearing ER+ tumor were treated with the competitive ER inhibitor fulvestrant 48 h prior to PET imaging with 18F-ETP. At 1 h post-injection time, static images were acquired and the tumor uptake values (%ID/g) were derived. Normal immature Sprague Dawley rats were used to perform biodistribution study. At 1 h post-injection of 18F-FES (1.85 MBq) or 18F-ETP (1.85 MBq), Sprague Dawley rats (n=5 in each group) were sacrificed. Tissues of interest were weighed and counted in a γ-counter.
**Results**: 18F-ETP was successfully synthesized, characterized and radiolabeled. Typical radiochemical synthesis time including HPLC purification was about 60 min with good decay-corrected yield (40–60%). After HPLC purification, 18F-ETP was obtained with high specific activity (≥100 GBq/μmol) and high radiochemical purity (≥99%). The results of in vitro stability study of 18F-ETP showed excellent stability both in serum and saline after incubation for 4 h. Octanol/water partition coefficient of 18F-ETP is 0.23 (log P), indicate it has much better hydrophilicity than that of 18F-FES (log P = 2.81). The cell uptake study revealed that 18F-ETP binds strongly to ER-positive MCF-7 cells (22.11% ± 4.27% of probe uptake at 1 h of incubation), and binds weakly to ER-negative MDA-MB-231 cells (0.43% ± 0.01% of probe uptake at 1 h of incubation). The blocking study showed that the specific binding of 18F-ETP could be blocked in the presence of 10 μg of estradiol (0.41% ± 0.083% of probe uptake at 1 h of incubation). The biodistribution results of 18F-ETP in normal SD rats displayed high uterus uptake at 1 h post-injection time (8.55±1.21%ID/g for intravenous injection and 6.83±1.70%ID/g for intraperitoneal injection), which higher than that of 18F-FES (3.92±2.39%ID/g for intravenous injection and 5.09±1.79%ID/g for intraperitoneal injection). While for the blocking studies, the uptake of uterus was obviously inhibited (0.68±0.26%ID/g). As expected, the micro-PET/CT imaging showed that 18F-ETP had considerable uptakes in ER positive MCF-7 tumor (3.27±0.19%ID/g) with a relatively high tumor-to-muscle ratio (3.36±0.02) and could be blocked thoroughly (1.00±0.089%ID/g). By contrast, 18F-ETP had low uptake in ER negative MDA-MB-231 (1.09±0.08%ID/g) tumor. Meanwhile, 18F-FES showed relatively low uptake in MCF-7 tumor (0.14±0.01%ID/g).
**Conclusion**: We developed a novel estradiol-based ER probe named 18F-ETP, which shows high radiochemical yield and has good stability in serum and normal saline. Compared with 18F-FES, 18F-ETP has a lower lipophilicity which may decreases the liver metabolism and non-target tissue uptake, leads to better target-to-nontarget ratios. 18F-ETP showed favorable characteristics in vitro and promising properties in vivo with specific ER positive tumor uptake and good tumor to background contrast, making it a potent candidate for ER imaging with PET.



## Preliminary Discussion about 11C-HED PET/CT in the Diagnosis of Pheochromocytoma and Paraganglioma

Haonan YU[1], Jiang LI[2], Qiu song CHEN[1]*
[1] *Department of PET-CT Diagnostic, Tianjin Medical University General Hospital, Tianjin, People's Republic of China*
[2] *Department of Urology, Tianjin Medical University General Hospital, Tianjin, People's Republic of China*

**Objective**: 11C-Hydroxyephedrine (11C-HED) is a catecholamine substrate analog, which concentrates in adrenergic nerve terminals. The purposes of this investigation were to characterize the uptake of 11C-HED in PHEO and to evaluate the diagnostic value of 11C-HED PET/CT compare with 18F-FDG PET/CT.
**Methods**: 22 patients suffering from hypertension and had a mass in adrenal or retroperitoneal region suspected PHEOs or PGLs were adopted. Each patient underwent PET/CT scanning with 18F-FDG and 11C-HED. Final diagnosis was based on histopathological evaluation. The sensitivity, specificity, and accuracy were counted for both two scans.
**Results**: The histological results were: adrenal pheochromocytoma (n=7), adrenal adenoma (n=6), adrenal lymphoma (n=1), adrenal malignant nerve sheath tumor(n=1), adrenal hematoma (n=2), liver cancer hepatocellular carcinoma (n=1, involve the right adrenal gland), retroperitoneal paraganglioma (n=3), retroperitoneal nerve sheath tumor (n=1). The sensitivity, specificity, and accuracy for identifying of the tumor nature were 90.0% (9/10), 66.7% (8/12), and 77.2% (17/22) for 18F-FDG PET/CT, and 100.0% (10/10), 91.7% (11/12), and 95.5% (21/22) for 11C-HED PET/CT, respectively.
**Conclusion**: Carbon-11 labeled radio-tracers show great potential clinical value since relatively limited patient radioactive exposure. 11C-HED is a useful modality to identify the PHEOs and PGLs in the clinical strategy.

P_124

## Synthesis and Evaluation of 18F Labeled Antisense Oligonucleotide Targeting Tumor Overexpressed miRNA

Lei Kang[1], Yan Huo[1], Rongfu Wang[1], Xiaojie Xu[2]
*[1] Peking University First Hospital, Beijing 100034, China;*
*[2] Academy of Military Medical Sciences, Beijing 100850, China*

**Objective**: We explored the optimized methods in the preparation of 18F radiolabeled AMO-155 with further in vitro evaluation.
**Methods**: The probe was radiolabelled with 18F using a direct Al18F labeling method. After conjugated with NOTA via an amine linker of NH2 and six carbon, Different reaction conditions were evaluated by HPLC for optimization. The product was identified by gel electrophoresis and gel imaging. Its serum stability and cellular uptake in MCF-7 cells were evaluated.
**Results**: Increasing the temperature in conjugation could improve the conjugated yield from 15% to 47%. The labeling is typically done at 100 °C for 15 min and the labeling efficiency reached to nearly 98%. The radiochemical purity of 18F-AMO in fresh human serum at 37 °C could maintain more than 95% during 6 h. The gel electrophoresis result showed that the location of radioactivity, which was imaged by micro-PET, coincided with the position of the AMO band and there was no degradation. The cellular uptake of 18F-AMO increased from 9% to 57% during the incubation of 6 h, whereas that of 18F did not increase significantly.
**Conclusion**: 18F labeled probe has a good serum stability and could be prepared easily and simply for in vivo imaging without further purification.

P_125

## Comparison Between 99mTc Radiolabeled siRNA Singlet and Duplex in Serum Stability and Cellular Uptake by HepG2 Cells

Lei Kang[1], Xiaojie Xu[2], Rongfu Wang[1], Ping Yan[1], Chunli Zhang[1]
*[1] Peking University First Hospital, Beijing 100034, China;*
*[2] Academy of Military Medical Sciences, Beijing 100850, China*

**Objective**: This study was to compare the stability and activity between 99mTc labeled siRNA singlet and duplex in vitro.
**Methods**: The 21mer antisense RNAs were conjugated with bifunctional chelator S-Acetyl NHS-MAG3. The labeling efficiencies under different reaction conditions including reaction time and input of SnCl2·2H2O were evaluated. The serum stability and HepG2 cellular uptake was investigated at different time points.
**Results**: The labeling efficiency reached 73.4%±3% (n=5) at room temperature, and the RNA recovery rate was always higher than 98%. In the incubation in fresh serum for 6h, the radiochemical purity of labeled duplex was no less than 90%, while that of singlet decreased to 76.4% in room temperature. The gel electrophoresis result showed more degradation of singlet probes than the duplex probes, especially at 6h. The uptake of 99mTc-duplex by HepG2 cells with and without liposome transfection increased quickly within 6 hours, and reached maximum separately 50.22±2.6% and 32.86±3.1% (n=4). However the uptake of 99mTc-singlet attained similar ratios compared to the duplex. There existed no significant difference in the cellular uptake between them (P>0.05).
**Conclusions**: 99mTc-siRNA duplex showed higher serum stability than the 99mTc-singlet RNA, suggesting more suitable for the in vivo usage, while they have a similar cellular affinity.

P_126

## Diagnostic Value of Fluorine-18 Fluorodeoxyglucose Positron Emission Tomography Computed Tomography in Fever of Unknown Origin

Lei Kang[1], Xiaojie Xu[2], Rongfu Wang[1], Yan Fan[1], Zhanli Fu[1]
*[1] Peking University First Hospital, Beijing 100034, China;*
*[2] Academy of Military Medical Sciences, Beijing 100850, China*

**Objective**: Fever of unknown origin (FUO) is a challenging problem in diagnosis in clinic. This study is to evaluate the diagnostic value of 18F-FDG PET/CT in FUO.
**Methods**: We analyzed the records of 51 patients with FUO retrospectively. All patients were examined by 18F-FDG PET/CT and the results were compared to the final diagnosis established by additional procedures including pathology, laboratory examination and clinical follow-up for more than 3 months. The maximum of standard uptake value (SUVmax) in tumors and benign lesions was compared. T test was used for statistical analysis.
**Results**: Final diagnosis were established for 48 patients, including 31 patients with infectious diseases, 9 with malignancies, and 8 with non-infectious inflammatory diseases. By FDG PET alone, the true positive (TP), false positive (FP), false negative (FN) and true negative (TN) rate was 52.9%, 27.5%, 17.6% and 2.0%, respectively. By FDG PET/CT, TP, FP, FN and TN rate was 70.6%, 27.5%, 2.0% and 0%, respectively. PET/CT had a sensitivity of 97.3% (36/37), a specificity of 0% (0/14) and an accuracy of 70.6% (36/51) in FUO, especially a high sensitivity and accuracy of 100% (9/9) in malignant tumor.
**Conclusions**: 18F-FDG PET/CT is a valuable imaging tool for the identification of the etiology in patients with FUO.

P_127

## Application of Quantitative Dynamic Whole-Body 18FDG-PET/CT in the differential Diagnosis of Pulmonary Nodules

Jianhua Zhang, Qian Wu, Rongfu Wang, Yan Fan, Zhanli Fu, Xuchu Zhang, Meng Liu, Lijuan Di, Yanfu Wang, Guangyu Zhao
*Nuclear Medicine Department at Peking University First Hospital, Beijing, China*

**Objectives**: To develop the non-invasive techniques to measure plasma input function and to investigate the cut-off value between malignant and benign lung nodules and to compare the diagnostic efficiency of dynamic whole body PET/CT and routine PET/CT.
**Material and methods**: Dynamic whole-body PET/CT scanning followed by a routine examination was performed on 30 patients suspected with lung nodules. The final diagnosis was based on pathological results. Image derived input function method would be developed and validated in the novel context of whole body dynamically-acquired images. Patlak plot method was used to acquire Ki (FDG influx rate constant). Receiver operating characteristic curve method was used to generate the Ki cut-off value for differentiating benign and malignant lesions.
**Results**: Plasma input function got from mean value of ascending and descending aorta between 30~60 min , corrected by population-based input function , was the best method in our study. Of the 52 lesions in all 30 patients, 45 lesions were malignant and the other 7 lesions were benign. Ki of benign lesions and malignant lesions were 1.0765±0.68403 and 1.9376±1.05668 respectively , area under ROC curve was 0.756. when cut-off value of Ki was 0.9628, the sensitivity and specificity was 80% and 57.1%, respectively. According to the Spearman correlation analysis, the correlation coefficient between SUVmax and Ki was r = 0.748, R2 = 0.532 ( $P<0.05$ ) . Of all the 52 lesions, dynamic whole-body PET/CT was correctly associated 50 lesions, except for 2 false positive lesions. Meanwhile, conventional PET/CT revealed 4 false positive lesions. The sensitivity, specificity and accuracy of dynamic whole-body PET/CT and routine PET/CT were 100%, 71.4%, 96.2% and 100%, 43%, 92.3%, respectively.
**Conclusions**: Quantitative dynamic whole-body 18F-FDG PET/CT is feasible and these preliminary data suggest it to be superior to conventional 18F-FDG PET/CT in lung nodule characterization, Ki (0.9628) may be as an appropriate cut-off value to differentiate the malignant and benign lesions.

2016 ARCCNM/CJK
15th Annual General Meeting of the Asian Regional Cooperative Council for Nuclear Medicine
7th CJK Conference on Nuclear Medicine

Jul. 15, 2016
Sheraton Shenyang South City Hotel, Shenyang, China

**Asian Regional Cooperative Council for Nuclear Medicine**
6F Saehan Bldg. 106, Nambusunhwan-ro 356-gil, Seocho-gu, Seoul, 137-888, Korea
Tel:+82-70-8867-7996
Fax:+82-303-3441-7996
E-mail: arccnm@arccnm.org,
Homepage: http://arccnm.org

**The Chinese Society of Nuclear Medicine**
No.155 North Nanjing Street, Heping District,
Shenyang, Liaoning Province, China
Tel: +86-24-8328-2142
Fax: +86-24-8328-2671
E-mail: ymli2001@163.com
Homepage: http://www.chinanm.org.cn

*Edited by Trinity Communications, Co., Ltd*
*E-mail: comms.trinity@gmail.com*